



# Synthesis of high quality silver nanowires and their applications in ultrafast photonics

W. J. LIU,<sup>1,2</sup> M. L. LIU,<sup>1</sup> S. LIN,<sup>1,3</sup> J. C. LIU,<sup>1,3</sup> M. LEI,<sup>1,5</sup> H. WU,<sup>3</sup> C. Q. DAI,<sup>4,6</sup> AND Z. Y. WEI<sup>2,\*</sup>

<sup>1</sup>State Key Laboratory of Information Photonics and Optical Communications, School of Science, P. O. Box 122, Beijing University of Posts and Telecommunications, Beijing 100876, China

<sup>2</sup>Beijing National Laboratory for Condensed Matter Physics, Institute of Physics, Chinese Academy of Sciences, Beijing 100190, China

<sup>3</sup>State Key Laboratory of New Ceramics and Fine Processing, School of Materials Science and Engineering, Tsinghua University, Beijing 100084, China

<sup>4</sup>Zhejiang A&F University, School of Science, Linan 311300, Zhejiang, China

<sup>5</sup>mlei@bupt.edu.cn

<sup>6</sup>dcq424@126.com

\*zywei@iphy.ac.cn

**Abstract:** Silver nanowires are widely used in catalysts, surface enhanced Raman scattering, microelectronic equipment, thin film solar cells, microelectrodes and biosensors for their excellent conductivity, heat transfer, low surface resistance, high transparency and good biocompatibility. However, the optical nonlinearity of silver nanowires has not been further explored yet. In this paper, three silver nanowire samples with different concentrations are produced via a typical hydrothermal method. Their applications to fiber lasers are implemented to prove the optical nonlinearity of silver nanowires for the first time. Based on three kinds of silver nanowires, the mode-locked operation of fiber lasers is successfully realized. Moreover, the fiber laser based on the silver nanowire with a concentration of 2 mg/L demonstrates the shortest pulse duration of 149.3 fs. The experiment not only proves the optical nonlinearity of silver nanowires, but also has some enlightenment on the selection of the optimum concentration of silver nanowires in the consideration of ultrashort pulse output.

© 2019 Optical Society of America under the terms of the [OSA Open Access Publishing Agreement](#)

## 1. Introduction

As one of the one-dimensional nanomaterials, the silver nanowire (AgNW) presents the characteristics different from the macroscopic silver or single silver atoms in the aspects of interface effect, small size effect, macroscopic quantum tunneling effect, quantum size effect and dielectric constraint effect [1]. The AgNW has been widely concerned in recent years due to their excellent conductivity, heat transfer, low surface resistance, high transparency and good biocompatibility [1–4]. It not only has outstanding performance in catalysis and biosensors, but also promotes the development of wearable devices as flexible conductive materials [5–9]. In addition, AgNW has been applied to surface enhanced Raman scattering in optical field. However, the optical nonlinearity of AgNW has not been further explored yet.

On the other hand, ultrafast fiber lasers have increasingly become the wide range of commercial and scientific options due to their irreplaceable inherent technological superiority, such as high efficiency, easy operation, power scalability and robustness [10–13]. Relying on passively mode-locked technology and diverse saturable absorbers (SAs), ultrafast fiber lasers have made great achievements so far. With the progress of technology, the type of SA has also changed from the early expensive semiconductor saturable absorber mirror (SESAM) [14,15] to the recent high-performance nanomaterials, such as graphene [16–20], transition metal dichalcogenides (TMDs) [21–29], black phosphorus (BPs) [30–34] and topological insulators (TIs) [35–39]. Although those materials have made significant breakthroughs in achieving ultrafast pulses, our efforts to find new and more efficient SA have not stopped.

In view of the outstanding performance of AgNW in the fields of electricity, heat, magnetism and catalysis, we are trying to find out whether it performs optical nonlinearity in optics field. It is a simple and effective way to prove the optical nonlinearity of AgNW with the aid of fiber lasers. Because of the optical nonlinearity of AgNW, it can be used as an ultrafast optical switch to achieve optical pulse shaping [40–43]. Generally speaking, there are two parameters to determine the saturable absorber performance of a material: relaxation time and third-order nonlinear polarizability [44]. During the relaxation process, the fast relaxation time is the main factor affecting the shaping ability of pulses [45,46]. It has reported that the relaxation time of AgNW is shorter than that of graphene [47]. This result indicates that the potential of AgNW to produce ultrashort pulses is comparable to that of graphene. Similarly, the third-order nonlinear polarizability has been proved with the Z-scan technique [48]. By comparison, the nonlinear refractive index of AgNW is comparable to or even better than that of TMDs. In summary, AgNW has a satisfactory performance in both relaxation time and nonlinearity.

In this paper, the optical nonlinearity of AgNW is proved experimentally. The mode-locked Er-doped fiber (EDF) laser based on AgNW is implemented. The AgNW is synthesized via a typical hydrothermal method. To explore whether the solution concentration has an effect on the performance of the EDF laser, the comparative experiments are implemented with three solutions of different concentration under the same conditions. By comparison, the EDF laser based on the AgNW with the concentration of 2 mg/L performs best in terms of ultrashort pulse output. The shortest pulse duration is 149.3 fs.

## 2. Preparation and characterization

In this work, AgNW was synthesized via a typical hydrothermal method [49]. As shown in Fig. 1(a), silver nitrate ( $\text{AgNO}_3$ ), polyvinylpyrrolidone (PVP), and copper chloride dihydrate ( $\text{CuCl}_2 \cdot 2\text{H}_2\text{O}$ ) were mixed together and stirred for 10 min to form precursor solution. After 3h of 130 °C heating, AgNW was obtained. Surface metallization modification of the fiber connector was then performed via 1500 rpm spin coating using AgNW/EtOH solution in Fig. 1(a). The surface color of fiber connector remained white after naturally drying, owing to the slender diameter and low fill-factor of AgNW in Fig. 1(b). Figure 1(c) indicates the diameter distribution of AgNW. In order to collect the crystallographic information of as-prepared AgNW, X-ray diffraction (XRD) was employed. Results show three characteristic peaks from  $2\theta = 30$  to 70 degrees, corresponding to (111), (200), and (220) crystal faces of silver in Fig. 1(d). There is no other diffraction peak attended, indicating the highly purity of as-prepared AgNW. X-ray photoelectron spectroscopy (XPS) peak-differentiation-imitating analysis around Ag3d region showed well separated spin-orbit components with a gap of 6.0 eV in Fig. 1(e), which also prove that the exist of metallic silver rather than silver nitrate residue or silver oxide [50,51]. The left one of Fig. 1(f) is the image of fiber end face without AgNW. The right one of Fig. 1(f) is fiber end face with AgNW.

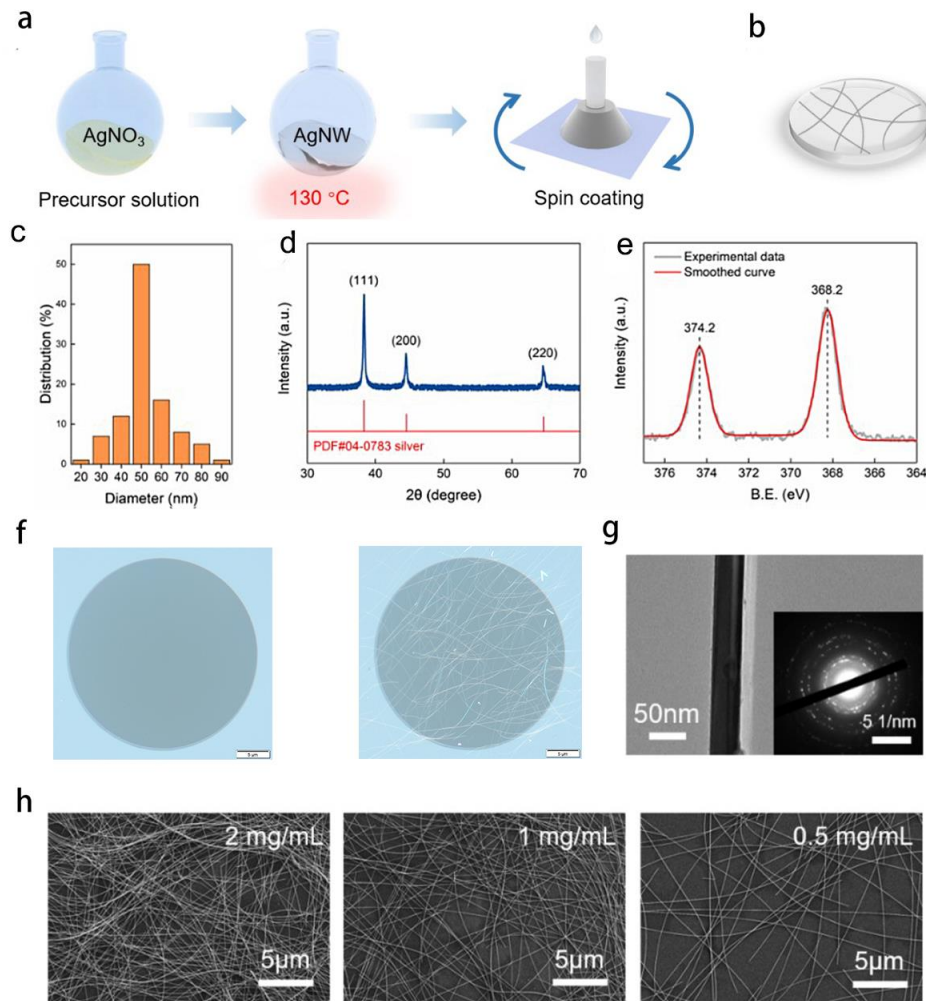


Fig. 1. Preparation process and characterization of AgNW. (a) Preparation of AgNW SA, (b) The surface of AgNW SA with low fill-factor, (c) The diameter distribution of AgNW, (d) XRD, (e) XPS, (f) Fiber end face with or without AgNW, (g) TEM, (h) AgNW coating layer with different concentration of AgNW from 2 mg/L to 0.5 mg/L.

It can be seen that the AgNW is attached to the effective area of the optical fiber. Micromorphologies of AgNW were characterized via a transmission electron microscope (TEM) and a scanning electron microscope (SEM). High-resolution TEM image also shows uniform nanowire structure of AgNW with a diameter of  $\sim 50$  nm in Fig. 1(g). Selected area electron diffraction (SAED) reveals a polycrystalline ring, backing well the XRD diffraction result provided before. Surface metal fill-factor is a critical factor in the laser response. By controlling the concentration of AgNW in AgNW/EtOH solution, different fill-factor AgNW coating were obtained. To further explore and contrast the mode locking performances of fiber connectors, AgNW coating layer with different concentration of AgNW from 2 mg/L to 0.5 mg/L were pre-prepared on three fiber connectors in Fig. 1(h).

To characterize the nonlinear saturable absorption properties of AgNW, the double-balanced detection method was adopted. The beam from the laser source was divided into two parts, one passing through the AgNW SA and the other passing through the single-mode fiber as a reference. By changing the power of the light, the relationship between the power intensity and transmittance of the AgNW SA is revealed. As shown in Fig. 2, three

AgNW SAs with different concentrations have great disparity in the nonlinear absorption properties. The curve in Fig. 2 is fitted by the following formula,

$$T = \frac{\alpha_s}{1 + I/I_{sat}} + \alpha_{ns},$$

where  $T$  is the transmittance,  $\alpha_s$  is the saturable loss,  $\alpha_{ns}$  is the non-saturable loss,  $I$  is the input intensity, and  $I_{sat}$  is the saturation intensity. The AgNW SA with concentration of 2 mg/L exhibits the maximum modulation depth of 59.5% among three SAs as shown in Fig. 2(a). The modulation depth of the AgNW SA with concentration of 1 mg/L and 0.5 mg/L decrease in turn, which are given as 34.19% and 21.1%, respectively.

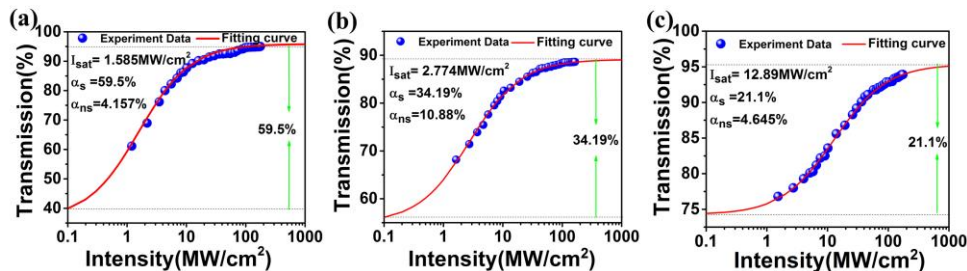


Fig. 2. (a) Nonlinear saturable absorption of AgNW with concentration of 2 mg/L, (b) Nonlinear saturable absorption of AgNW with concentration of 1 mg/L, (c) Nonlinear saturable absorption of AgNW with concentration of 0.5 mg/L.

### 3. Experiment

In order to confirm the optical nonlinearity of AgNW, we have adopted the traditional EDF ring laser. The construction of the proposed nonlinear optical verification device based on AgNW is shown in Fig. 3. The laser diode (LD) which pump EDF (0.6 m) through a wavelength division multiplexer (WDM, 980/1550 nm) operated at 980 nm with the maximum power of 630 mW. The isolator (ISO) is employed to guarantee unidirectional light propagation. By carefully adjust the polarization controller (PC), the polarization state and operation state will be optimized to a certain extent. By means of a 20% fiber coupler, the real-time status of the cavity can be monitored by the test equipment. The corresponding pulse profile, spectrum, frequency spectrum is identified by oscilloscope (Tektronix DPO3054), optical spectrum analyzer (Yokogawa AQ6370C) and RF spectrum analyzer (Agilent E4402B), respectively.

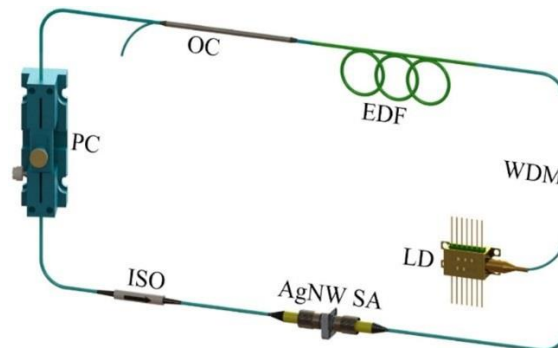


Fig. 3. Construction of the EDF laser based on the AgNW SA.

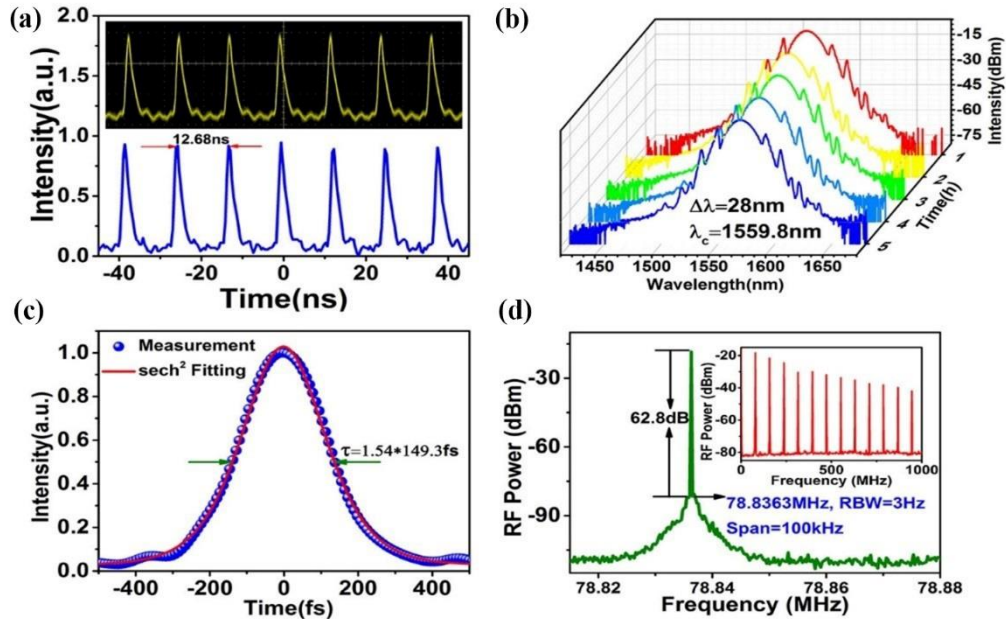


Fig. 4. (a) Oscilloscope trace, (b) Spectrum, (c) Autocorrelation trace, (d) RF spectrum.

#### 4. Result and discussion

To explore whether solution concentration has an effect on the performance of EDF lasers, three different AgNW concentrations are adopted to conduct experiments. In the first experiment, the AgNW SA with concentration of 2 mg/L is used, and the corresponding laser performances are summed up in Fig. 4. The mode-locking operation is realized when the pump power run up to 160 mW. As shown in Fig. 4(a), the pulse interval is 12.68 ns observed from the oscilloscope trace. The long-time output spectrum is demonstrated in Fig. 4(b). Obviously, there are some sidebands on both sides of the spectrum, which is the characteristic spectrum of standard soliton mode-locking. The EDF laser based on the AgNW SA with the concentration of 0.5 mg/L operates at 1559.8 nm with the bandwidth of 28 nm. As shown in Fig. 4(c), the autocorrelation trace is revealed consistent well with the track of  $\text{sech}^2$  function, which corresponds the pulse duration of 149.3 fs. The corresponding time bandwidth product of realized EDF laser is calculated as 0.5151, which indicates that the whole mode-locking system is slightly chirped. Meanwhile, the corresponding radio frequency (RF) spectrum with the span of 100 kHz and resolution of 3 Hz is shown in Fig. 4(d). The fundamental repetition rate is 78.8363 MHz. The signal-to-noise ratio (SNR) is measured as 62.8 dB, which illustrates the exceptional stability of the mode-locking operation. The inset in Fig. 4(d) reveals the frequency multiplication spectrum measured in the wide span of 1000 MHz. The calculated maximum pulse energy and optical damage threshold of the SAs is 328.52  $\mu\text{J}$  and 0.515  $\text{mJ}/\text{cm}^2$ , respectively.

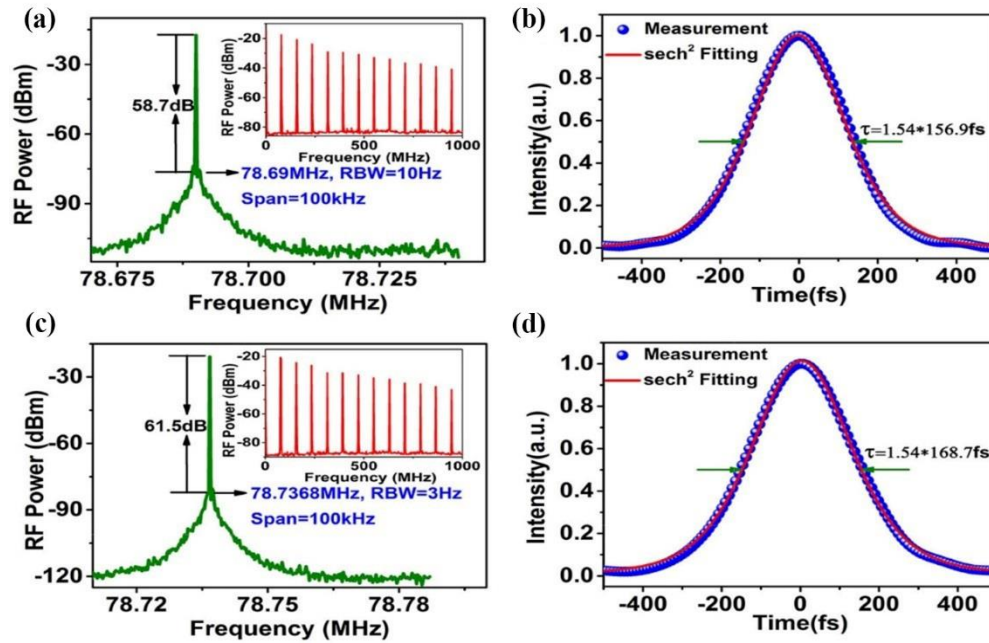


Fig. 5. The spectrum (a) and autocorrelation trace (b) of AgNW with concentration of 1 mg/L. The spectrum (c) and autocorrelation trace (d) of AgNW with concentration of 0.5 mg/L.

Table 1. The EDF laser performance based on AgNW with different concentrations.

Material	MD (%)	$\lambda_c/\Delta\lambda$ (nm)	$\tau$ (fs)	SNR(dB)	P(mW)
AgNW(2mg/L)	55.42	1559.8/28	149.3	62.8	25.9
AgNW(1mg/L)	34.19	1559.8/27	156.9	58.7	26.5
AgNW(0.5mg/L)	22.1	1557.4/26	168.7	61.5	22.8

Table 2. Comparison of mode-locked EDF lasers based on different nonlinear optical materials.

Materials	Preparation method	$\tau$ (fs)	SNR(dB)	$\lambda_c/\Delta\lambda$ (nm)	MD (%)	IL	P(mW)	Refs.
CNTs	EAD	66	58	1555/54	7.8	1.94	26	[52]
Graphene	CVD	88	65	1545/48	4.8	1.6	1.5	[53]
Bi <sub>2</sub> Se <sub>3</sub>	Polyol	660	55	1557.5/4.3	3.9	4.88	–	[54]
Sb <sub>2</sub> Te <sub>3</sub>	ME	1800	60	1558.6/1.8	–	–	0.5	[55]
BPs	ME	946	70	1571.45/2.9	8.1	1.67	–	[56]
WS <sub>2</sub>	PLD	246	92	1561/57	25.48	3.77	18	[38]
MoS <sub>2</sub>	CVD	1280	62	1568.9/2.6	35.4	1.67	5.1	[57]
MoSe <sub>2</sub>	LPE	737	61.9	1557.3/5.4	5.4	1.25	3.96	[58]
WSe <sub>2</sub>	liquid exfoliation	1310	50	1556.7/2	0.3	2.77	0.45	[59]
AgNW	hydrothermal method	149.3	62.8	1559.8/28	59.5	0.184	25.9	This work

Subsequently, the AgNW with solution concentration of 1 mg/L and 0.5 mg/L are also successfully applied to the same laser. When the concentration of AgNW is 1 mg/L, the corresponding repetition rate and the pulse duration are 78.69 MHz and 156.9 fs as shown in Figs. 5(a) and 5(b). Analogously, the repetition rate and pulse duration of the EDF laser based on AgNW with the concentration of 0.5 mg/L are given as 78.7368 MHz and 168.7 fs in Figs. 5(c) and 5(d). More detailed data on three different mode-locked lasers are listed in Table 1. The contrast results show that the trend of concentration and pulse duration are not consistent. That result indicates that there exists an optimum concentration to achieve ultrafast pulse output.

In addition, the laser performance comparison of AgNW with the traditional SAs has also been implemented. The pulse duration of 149.3 fs in our experiment is shorter compared with most EDF lasers in Table 2. This not only proves the optical nonlinearity of AgNW, but also indicates it has great advantages in realizing ultrashort pulses.

## 5. Conclusion

In this paper, three AgNW samples with different concentrations have been prepared via a typical hydrothermal method. The characterization of three different SAs based on AgNW have indicated the high modulation depth and small insertion loss of them. In the experiment, three kinds of samples have been successfully applied in the EDF lasers. In addition, through the laser performance comparison of AgNW with different concentrations, it is found that there exists an optimum concentration in achieving short pulse output for AgNW. The pulse duration of 149.3 fs is also superior to most EDF lasers based on some classical materials. Our experiment not only demonstrates the optical nonlinearity of AgNW, but also enlightens that the AgNW with optimal concentration is competitive for the development and promotion of ultrafast mode-locked pulses.

## Funding

National Natural Science Foundation of China (NSFC) (11674036; 11875008); Beijing Youth Top-Notch Talent Support Program (2017000026833ZK08); Fund of State Key Laboratory of Information Photonics and Optical Communications (Beijing University of Posts and Telecommunications, IPOC2017ZZ05); State Key Laboratory of Advanced Optical Communication Systems and Networks, Shanghai Jiao Tong University (2019GZKF03007); Beijing University of Posts and Telecommunications Excellent Ph.D. Students Foundation (CX2019202).

## References

1. L. Hu, H. S. Kim, J. Y. Lee, P. Peumans, and Y. Cui, "Scalable coating and properties of transparent, flexible, silver nanowire electrodes," *ACS Nano* **4**(5), 2955–2963 (2010).
2. H. Dittlbacher, A. Hohenau, D. Wagner, U. Kreibig, M. Rogers, F. Hofer, F. R. Aussenegg, and J. R. Krenn, "Silver nanowires as surface plasmon resonators," *Phys. Rev. Lett.* **95**(25), 257403 (2005).
3. S. De, T. M. Higgins, P. E. Lyons, E. M. Doherty, P. N. Nirmalraj, W. J. Blau, J. J. Boland, and J. N. Coleman, "Silver nanowire networks as flexible, transparent, conducting films: extremely high DC to optical conductivity ratios," *ACS Nano* **3**(7), 1767–1774 (2009).
4. V. Scardaci, R. Coull, P. E. Lyons, D. Rickard, and J. N. Coleman, "Spray deposition of highly transparent, low-resistance networks of silver nanowires over large areas," *Small* **7**(18), 2621–2628 (2011).
5. S. Lin, X. Bai, H. Wang, H. Wang, J. Song, K. Huang, C. Wang, N. Wang, B. Li, M. Lei, and H. Wu, "Roll-to-roll production of transparent silver-nanofiber-network electrodes for flexible electrochromic smart windows," *Adv. Mater.* **29**(41), 1703238 (2017).
6. L. José Andrés, M. Fe Menéndez, D. Gómez, A. Luisa Martínez, N. Bristow, J. Paul Kettle, A. Menéndez, and B. Ruiz, "Rapid synthesis of ultra-long silver nanowires for tailor-made transparent conductive electrodes: proof of concept in organic solar cells," *Nanotechnology* **26**(26), 265201 (2015).
7. M. K. Oh, Y. S. Shin, C. L. Lee, R. De, H. Kang, N. E. Yu, B. H. Kim, J. H. Kim, and J. K. Yang, "Morphological and SERS properties of silver nanorod array films fabricated by oblique thermal evaporation at various substrate temperatures," *Nanoscale Res. Lett.* **10**(1), 962 (2015).
8. M. Amiri, S. Nouhi, and Y. Azizian-Kalandaragh, "Facile synthesis of silver nanostructures by using various deposition potential and time: A nonenzymatic sensor for hydrogen peroxide," *Mater. Chem. Phys.* **155**, 129–135 (2015).
9. A. R. Madaria, A. Kumar, and C. Zhou, "Large scale, highly conductive and patterned transparent films of silver nanowires on arbitrary substrates and their application in touch screens," *Nanotechnology* **22**(24), 245201 (2011).
10. R. Holzwarth, T. Udem, T. W. Hänsch, J. C. Knight, W. J. Wadsworth, and P. St. J. Russell, "Optical frequency synthesizer for precision spectroscopy," *Phys. Rev. Lett.* **85**(11), 2264–2267 (2000).
11. Z. Jiang, C. B. Huang, D. E. Leaird, and A. M. Weiner, "Optical arbitrary waveform processing of more than 100 spectral comb lines," *Nat. Photonics* **1**(8), 463–467 (2007).
12. F. Wang, A. G. Rozhin, V. Scardaci, Z. Sun, F. Hennrich, I. H. White, W. I. Milne, and A. C. Ferrari, "Wideband-tuneable, nanotube mode-locked, fibre laser," *Nat. Nanotechnol.* **3**(12), 738–742 (2008).

13. C. M. Eigenwillig, W. Wieser, S. Todor, B. R. Biedermann, T. Klein, C. Jirauschek, and R. Huber, "Picosecond pulses from wavelength-swept continuous-wave Fourier domain mode-locked lasers," *Nat. Commun.* **4**(1), 1848 (2013).
14. U. Keller, "Recent developments in compact ultrafast lasers," *Nature* **424**(6950), 831–838 (2003).
15. O. Okhotnikov, A. Grudinin, and M. Pessa, "Ultra-fast fibre laser systems based on SESAM technology: new horizons and applications," *New J. Phys.* **6**, 177 (2004).
16. A. P. Luo, P. F. Zhu, H. Liu, X. W. Zheng, N. Zhao, M. Liu, H. Cui, Z. C. Luo, and W. C. Xu, "Microfiber-based, highly nonlinear graphene saturable absorber for formation of versatile structural soliton molecules in a fiber laser," *Opt. Express* **22**(22), 27019–27025 (2014).
17. J. Sotor, J. Bogusławski, T. Martynkien, P. Mergo, A. Krajewska, A. Przewłoka, W. Strupieński, and G. Sobon, "All-polarization-maintaining, stretched-pulse Tm-doped fiber laser, mode-locked by a graphene saturable absorber," *Opt. Lett.* **42**(8), 1592–1595 (2017).
18. P. A. George, J. Strait, J. Dawlaty, S. Shivaraman, M. Chandrashekar, F. Rana, and M. G. Spencer, "Ultrafast optical-pump terahertz-probe spectroscopy of the carrier relaxation and recombination dynamics in epitaxial graphene," *Nano Lett.* **8**(12), 4248–4251 (2008).
19. H. Zhang, Q. L. Bao, D. Y. Tang, L. M. Zhao, and K. P. Loh, "Large energy soliton erbium-doped fiber laser with a graphene-polymer composite mode locker," *Appl. Phys. Lett.* **95**(14), 141103 (2009).
20. Z. Sun, T. Hasan, F. Torrisi, D. Popa, G. Privitera, F. Wang, F. Bonaccorso, D. M. Basko, and A. C. Ferrari, "Graphene mode-locked ultrafast laser," *ACS Nano* **4**(2), 803–810 (2010).
21. W. J. Liu, M. L. Liu, M. Lei, S. B. Fang, and Z. Y. Wei, "Titanium selenide saturable absorber mirror for passive Q-switched Er-doped fiber laser," *IEEE J. Sel. Top. Quantum Electron.* **24**(3), 1 (2018).
22. M. Zhang, R. C. T. Howe, R. I. Woodward, E. J. R. Kelleher, F. Torrisi, G. H. Hu, S. V. Popov, J. R. Taylor, and T. Hasan, "Solution processed MoS<sub>2</sub>-PVA composite for sub-bandgap mode-locking of a wideband tunable ultrafast Er:fiber laser," *Nano Res.* **8**(5), 1522–1534 (2015).
23. P. G. Yan, A. J. Liu, Y. S. Chen, H. Chen, S. C. Ruan, C. Y. Guo, S. F. Chen, I. L. Li, H. P. Yang, J. G. Hu, and G. Z. Cao, "Microfiber-based WS<sub>2</sub>-film saturable absorber for ultra-fast photonics," *Opt. Mater. Express* **5**(3), 479–489 (2015).
24. M. L. Liu, W. J. Liu, P. G. Yan, S. B. Fang, H. Teng, and Z. Y. Wei, "High-power MoTe<sub>2</sub>-based passively Q-switched erbium-doped fiber laser," *Chin. Opt. Lett.* **16**(2), 020007 (2018).
25. J. Wang, Z. Jiang, H. Chen, J. Li, J. Yin, J. Wang, T. He, P. Yan, and S. Ruan, "Magnetron-sputtering deposited WTe<sub>2</sub> for an ultrafast thulium-doped fiber laser," *Opt. Lett.* **42**(23), 5010–5013 (2017).
26. W. J. Liu, L. H. Pang, H. N. Han, Z. W. Shen, M. Lei, H. Teng, and Z. Y. Wei, "Dark solitons in WS<sub>2</sub> erbium-doped fiber lasers," *Photon. Res.* **4**(3), 111–114 (2016).
27. W. J. Liu, Y. N. Zhu, M. L. Liu, B. Wen, S. B. Fang, H. Teng, M. Lei, L. M. Liu, and Z. Y. Wei, "Optical properties and applications for MoS<sub>2</sub>-Sb<sub>2</sub>Te<sub>3</sub>-MoS<sub>2</sub> heterostructure materials," *Photon. Res.* **6**(3), 220–227 (2018).
28. J. Du, Q. Wang, G. Jiang, C. Xu, C. Zhao, Y. Xiang, Y. Chen, S. Wen, and H. Zhang, "Ytterbium-doped fiber laser passively mode locked by few-layer Molybdenum Disulfide (MoS<sub>2</sub>) saturable absorber functioned with evanescent field interaction," *Sci. Rep.* **4**(1), 6346 (2014).
29. H. Zhang, S. B. Lu, J. Zheng, J. Du, S. C. Wen, D. Y. Tang, and K. P. Loh, "Molybdenum disulfide (MoS<sub>2</sub>) as a broadband saturable absorber for ultra-fast photonics," *Opt. Express* **22**(6), 7249–7260 (2014).
30. J. Sotor, G. Sobon, W. Macherzynski, P. Paletko, and K. M. Abramski, "Black phosphorus saturable absorber for ultrashort pulse generation," *Appl. Phys. Lett.* **107**(5), 051108 (2015).
31. G. Hu, T. Albrow-Owen, X. Jin, A. Ali, Y. Hu, R. C. T. Howe, K. Shehzad, Z. Yang, X. Zhu, R. I. Woodward, T. C. Wu, H. Jussila, J. B. Wu, P. Peng, P. H. Tan, Z. Sun, E. J. R. Kelleher, M. Zhang, Y. Xu, and T. Hasan, "Black phosphorus ink formulation for inkjet printing of optoelectronics and photonics," *Nat. Commun.* **8**(1), 278 (2017).
32. J. Li, H. Luo, B. Zhai, R. Lu, Z. Guo, H. Zhang, and Y. Liu, "Black phosphorus: a two-dimension saturable absorption material for mid-infrared Q-switched and mode-locked fiber lasers," *Sci. Rep.* **6**(1), 30361 (2016).
33. S. Liu, Y. Zhang, L. Li, Y. Wang, R. Lv, X. Wang, Z. Chen, and L. Wei, "Er-doped Q-switched fiber laser with a black phosphorus/polymethyl methacrylate saturable absorber," *Appl. Opt.* **57**(6), 1292–1295 (2018).
34. L. Yun, "Black phosphorus saturable absorber for dual-wavelength polarization-locked vector soliton generation," *Opt. Express* **25**(26), 32380–32385 (2017).
35. S. Q. Chen, C. J. Zhao, Y. Li, H. H. Huang, S. B. Lu, H. Zhang, and S. C. Wen, "Broadband optical and microwave nonlinear response in topological insulator," *Opt. Mater. Express* **4**(4), 587–596 (2014).
36. Z. Q. Luo, C. Liu, Y. Z. Huang, D. D. Wu, J. Y. Wu, H. Y. Xu, Z. P. Cai, Z. Q. Lin, L. P. Sun, and J. Weng, "Topological-insulator passively Q-switched double-clad fiber laser at 2 μm wavelength," *IEEE J. Sel. Top. Quantum Electron.* **20**(5), 0902708 (2014).
37. J. Sotor, G. Sobon, K. Grodecki, and K. M. Abramski, "Mode-locked erbium-doped fiber laser based on evanescent field interaction with Sb<sub>2</sub>Te<sub>3</sub> topological insulator," *Appl. Phys. Lett.* **104**(25), 251112 (2014).
38. H. Liu, X. W. Zheng, M. Liu, N. Zhao, A. P. Luo, Z. C. Luo, W. C. Xu, H. Zhang, C. J. Zhao, and S. C. Wen, "Femtosecond pulse generation from a topological insulator mode-locked fiber laser," *Opt. Express* **22**(6), 6868–6873 (2014).
39. W. Liu, L. Pang, H. Han, W. Tian, H. Chen, M. Lei, P. Yan, and Z. Wei, "70-fs mode-locked erbium-doped fiber laser with topological insulator," *Sci. Rep.* **6**(1), 19997 (2016).
40. Z. Kang, M. Y. Liu, C. Tang, X. Xu, Z. Jia, G. Qin, and W. Qin, "Microfiber coated with gold nanorods as saturable absorbers for 2 μm femtosecond fiber lasers," *Opt. Mater. Express* **8**(12), 3841–3850 (2018).



41. Z. Kang, M. Y. Liu, Z. W. Li, S. Q. Li, Z. X. Jia, C. Z. Liu, W. P. Qin, and G. S. Qin, "Passively Q-switched erbium doped fiber laser using a gold nanostars based saturable absorber," *Photon. Res.* **6**(6), 549–553 (2018).
42. Z. Kang, Y. Xu, L. Zhang, Z. X. Jia, L. Liu, D. Zhao, Y. Feng, G. S. Qin, and W. P. Qin, "Passively mode-locking induced by gold nanorods in erbium-doped fiber lasers," *Appl. Phys. Lett.* **103**(4), 041105 (2013).
43. F. Wang, Y. Jing, Z. Kang, L. B. Zhou, Z. R. Li, M. Y. Liu, T. Wang, C. F. Yao, H. B. Chen, W. P. Qin, Z. A. Qiao, G. S. Qin, and C. F. Wu, "Mesoporous carbon nanospheres as broadband saturable absorbers for pulsed laser generation," *Adv. Opt. Mater.* **6**(16), 1800606 (2018).
44. Y. C. Chen, N. R. Ravikiran, L. S. Schadler, P. M. Ajayan, Y. P. Zhao, T. M. Lu, G. C. Wang, and X. C. Zhang, "Ultrafast optical switching properties of single-wall carbon nanotube polymer composites at 1.55  $\mu\text{m}$ ," *Appl. Phys. Lett.* **81**(6), 975–977 (2002).
45. H. Shi, R. Yan, S. Bertolazzi, J. Brivio, B. Gao, A. Kis, D. Jena, H. G. Xing, and L. Huang, "Exciton dynamics in suspended monolayer and few-layer  $\text{MoS}_2$  2D crystals," *ACS Nano* **7**(2), 1072–1080 (2013).
46. Q. L. Bao, H. Zhang, Z. H. Ni, Y. Wang, L. Polavarapu, Z. X. Shen, Q. H. Xu, D. Y. Tang, and K. P. Loh, "Monolayer graphene as a saturable absorber in a mode-locked laser," *Nano Res.* **4**(3), 297–307 (2011).
47. Q. Ding, Y. Shi, M. Chen, H. Li, X. Yang, Y. Qu, W. Liang, and M. Sun, "Ultrafast dynamics of plasmon-exciton interaction of Ag nanowire-graphene hybrids for surface catalytic reactions," *Sci. Rep.* **6**(1), 32724 (2016).
48. Y. P. Han, J. L. Sun, H. A. Ye, W. Z. Wu, and G. Shi, "Nonlinear refraction of silver nanowires from nanosecond to femtosecond laser excitation," *Appl. Phys. B* **94**(2), 233–237 (2009).
49. J. Jung, H. Lee, I. Ha, H. Cho, K. K. Kim, J. Kwon, P. Won, S. Hong, and S. H. Ko, "Highly stretchable and transparent electromagnetic interference shielding film based on silver nanowire percolation network for wearable electronics applications," *ACS Appl. Mater. Interfaces* **9**(51), 44609–44616 (2017).
50. I. Washio, Y. J. Xiong, Y. D. Yin, and Y. N. Xia, "Reduction by the end groups of poly (vinyl pyrrolidone): a new and versatile route to the kinetically controlled synthesis of Ag triangular nanoplates," *Adv. Mater.* **18**(13), 1745–1749 (2006).
51. Y. Xiong, I. Washio, J. Chen, H. Cai, Z. Y. Li, and Y. Xia, "Poly(vinyl pyrrolidone): a dual functional reductant and stabilizer for the facile synthesis of noble metal nanoplates in aqueous solutions," *Langmuir* **22**(20), 8563–8570 (2006).
52. Z. H. Yu, Y. G. Wang, X. Zhang, X. Z. Dong, J. R. Tian, and Y. R. Song, "A 66 fs highly stable single wall carbon nanotube mode locked fiber laser," *Laser Phys.* **24**(1), 015105 (2014).
53. J. Sotor, I. Pasternak, A. Krajewska, W. Strupinski, and G. Sobon, "Sub-90 fs a stretched-pulse mode-locked fiber laser based on a graphene saturable absorber," *Opt. Express* **23**(21), 27503–27508 (2015).
54. H. Liu, X. W. Zheng, M. Liu, N. Zhao, A. P. Luo, Z. C. Luo, W. C. Xu, H. Zhang, C. J. Zhao, and S. C. Wen, "Femtosecond pulse generation from a topological insulator mode-locked fiber laser," *Opt. Express* **22**(6), 6868–6873 (2014).
55. J. Sotor, G. Sobon, W. Macherzynski, P. Paletko, K. Grodecki, and K. M. Abramski, "Mode-locking in Er-doped fiber laser based on mechanically exfoliated  $\text{Sb}_2\text{Te}_3$  saturable absorber," *Opt. Express* **4**(1), 1–6 (2014).
56. Y. Chen, G. Jiang, S. Chen, Z. Guo, X. Yu, C. Zhao, H. Zhang, Q. Bao, S. Wen, D. Tang, and D. Fan, "Mechanically exfoliated black phosphorus as a new saturable absorber for both Q-switching and Mode-locking laser operation," *Opt. Express* **23**(10), 12823–12833 (2015).
57. H. Xia, H. Li, C. Lan, C. Li, X. Zhang, S. Zhang, and Y. Liu, "Ultrafast erbium-doped fiber laser mode-locked by a CVD-grown molybdenum disulfide ( $\text{MoS}_2$ ) saturable absorber," *Opt. Express* **22**(14), 17341–17348 (2014).
58. J. Koo, J. Park, J. Lee, Y. M. Jhon, and J. H. Lee, "Femtosecond harmonic mode-locking of a fiber laser at 3.27 GHz using a bulk-like,  $\text{MoSe}_2$ -based saturable absorber," *Opt. Express* **24**(10), 10575–10589 (2016).
59. D. Mao, X. She, B. Du, D. Yang, W. Zhang, K. Song, X. Cui, B. Jiang, T. Peng, and J. Zhao, "Erbium-doped fiber laser passively mode locked with few-layer  $\text{WSe}_2/\text{MoSe}_2$  nanosheets," *Sci. Rep.* **6**(1), 23583 (2016).